Journal of Pathology Informatics 13 (2022) 100144

Contents lists available at ScienceDirect

Journal of Pathology Informatics

journal homepage: www.elsevier.com/locate/jpi

Development and technical validation of an artificial intelligence model for quantitative analysis of histopathologic features of eosinophilic esophagitis

Luisa Ricaurte Archila [a], Lindsey Smith [b], Hanna-Kaisa Sihvo [c], Thomas Westerling-Bui [c], Ville Koponen [c], Donnchadh M. O'Sullivan [d,e], Maria Camila Cardenas Fernandez [d,e], Erin E. Alexander [e,f], Yaohong Wang [g], Priyadharshini Sivasubramaniam [a], Ameya Patil [a], Puanani E. Hopson [e,f], Imad Absah [e,f], Karthik Ravi [f], Taofic Mounajjed [a], Rish Pai [h], Catherine Hagen [a], Christopher Hartley [a], Rondell P. Graham [a], Roger K. Moreira [a,*]

[a] Department of Laboratory Medicine and Pathology, Mayo Clinic Rochester, MN, USA
[b] Aiforia Technologies, Worcester, MA, USA
[c] Aiforia Technologies, Helsinki, Finland
[d] Department of Pediatric and Adolescence Medicine, Mayo Clinic Rochester, MN, USA
[e] Department of Gastroenterology and Hepatology, Mayo Clinic Rochester, MN, USA
[f] Division of Pediatric Gastroenterology and Hepatology, Mayo Clinic Rochester, MN, USA
[g] Department of Pathology, Vanderbilt University Medical Center, Nashville, TN, USA
[h] Department of Laboratory Medicine and Pathology, Mayo Clinic Scottsdale, AZ, USA

ARTICLE INFO

Keywords:
Artificial intelligence
Digital pathology
Eosinophilic esophagitis
Deep learning
EoE
Eosinophils

ABSTRACT

Background: In an attempt to provide quantitative, reproducible, and standardized analyses in cases of eosinophilic esophagitis (EoE), we have developed an artificial intelligence (AI) digital pathology model for the evaluation of histologic features in the EoE/esophageal eosinophilia spectrum. Here, we describe the development and technical validation of this novel AI tool.

Methods: A total of 10 726 objects and 56.2 mm^2 of semantic segmentation areas were annotated on whole-slide images, utilizing a cloud-based, deep learning artificial intelligence platform (Aiforia Technologies, Helsinki, Finland). Our training set consisted of 40 carefully selected digitized esophageal biopsy slides which contained the full spectrum of changes typically seen in the setting of esophageal eosinophilia, ranging from normal mucosa to severe abnormalities with regard to each specific features included in our model. A subset of cases was reserved as independent "test sets" in order to assess the validity of the AI model outside the training set. Five specialized experienced gastrointestinal pathologists scored each feature blindly and independently of each other and of AI model results.

Results: The performance of the AI model for all cell type features was similar/non-inferior to that of our group of GI pathologists (F1-scores: 94.5–94.8 for AI vs human and 92.6–96.0 for human vs human). Segmentation area features were rated for accuracy using the following scale: 1. "perfect or nearly perfect" (95%–100%, no significant errors), 2. "very good" (80%–95%, only minor errors), 3. "good" (70%–80%, significant errors but still captures the feature well), 4. "insufficient" (less than 70%, significant errors compromising feature recognition). Rating scores for tissue (1.01), spongiosis (1.15), basal layer (1.05), surface layer (1.04), lamina propria (1.15), and collagen (1.11) were in the "very good" to "perfect or nearly perfect" range, while degranulation (2.23) was rated between "good" and "very good".

Conclusion: Our newly developed AI-based tool showed an excellent performance (non-inferior to a group of experienced GI pathologists) for the recognition of various histologic features in the EoE/esophageal mucosal eosinophilia spectrum. This tool represents an important step in creating an accurate and reproducible method for semi-automated quantitative analysis to be used in the evaluation of esophageal biopsies in this clinical context.

Introduction

The histopathological features of eosinophilic esophagitis (EoE) have been well characterized since the earliest series describing this disease.[1,2] Eosinophil-rich infiltrate (currently defined as >15 eosinophils per high power field) represents the only required histopathological feature for this clinical–pathologic diagnosis.[3] However, several additional abnormalities are usually present on routine histologic examination, including lymphocytic inflammation (LI) (often representing the predominant inflammatory cell type), eosinophilic abscesses (EA), basal zone hyperplasia (BZH), dilated

* Corresponding author at: 200 1st St. SW, Hilton Building, Anatomic Pathology, Rochester, MN 55905, USA.
E-mail address: Moreira.roger@mayo.edu (R.K. Moreira).

http://dx.doi.org/10.1016/j.jpi.2022.100144
Received 31 August 2022; Received in revised form 16 September 2022; Accepted 22 September 2022
Available online 27 September 2022

intercellular spaces (DIS), dyskeratosis (DK), surface epithelial change (SEC), and lamina propria fibrosis (LPF).[4,5]

Peak eosinophil count (PEC) represents the most commonly reported histopathological parameter in the context of esophageal mucosal eosinophilia, whereby pathologists identify the area of highest concentration of eosinophils within a given sample and count the number of eosinophils within 1 high power field by unaided (i.e., without digital tools) visual inspection through routine light microscopy. Recently, a more comprehensive semi-quantitative method – the eosinophilic esophagitis histologic scoring system (EoEHSS) – has been developed and validated.[5–7] In addition to the assessment of eosinophils, this method also includes semi-quantitative scoring of various features of epithelial injury.

Although the EoEHSS has advantages over PEC alone, it does have some important limitations, including the use of semi-quantitative (rather than quantitative) assessment of various features, being significantly more time-consuming and labor-intensive than PEC, and the continued susceptibility to various measurement errors related to various factors. These include the intrinsic difficulties in selecting areas of highest eosinophil concentration within a sample, with properly counting eosinophils, and with dealing with the marked variation in the HPF area of different microscopes (by various manufacturers) commonly used by pathologists.

In view of the shortcomings of currently utilized systems, and to provide quantitative, reproducible, and standardized analyses, we have developed a novel artificial intelligence (AI)-based digital pathology model for the evaluation of histologic features in the spectrum of EoE (and esophageal eosinophilia more broadly). In this study, we describe the development, validation, features, and functionality of this AI model in detail.

Materials and methods

Model description and development

Our model was developed utilizing whole-slide images and a cloud-based, supervised deep learning artificial intelligence platform (Aiforia Technologies, Helsinki, Finland). All slides were scanned at × 40 magnification on the Aperio ScanScope AT Turbo brightfield instrument (Leica Biosystems) at a resolution of 0.25 μm per pixel and uploaded to the Aiforia platform. Our training set consisted of 40 carefully selected digitized esophageal biopsy slides which contained the full spectrum of changes typically seen in the setting of esophageal eosinophilia, ranging from normal mucosa to severe abnormalities (with regard to each specific feature included in our model).

The AI model was trained as a set of nested individual convolutional neural networks (CNN), called "layers". The individual CNNs were trained independently of each other, but were executed in a progressive fashion so that the topmost (parental) CNN first analyzed the slide and only the areas identified were subsequently analyzed by the following CNN (1st child), and so on. Each individual layer was designed to identify a single or multiple classifiers, called "classes", and annotations were provided as training data for each class within a given layer. Our AI model was comprised of 5 layers, with each layer having a specific set of classes (total of 10), as shown in Table 1.

A total of 10 726 objects (including 1255 eosinophils, 8766 squamous cell nuclei, and 705 lymphocytes) and 56.2 mm^2 of semantic segmentation areas (including 32 mm^2 of "tissue", 9.1 mm^2 of "tissue sublevels", 0.05 mm^2 of "intercellular edema/DIS", 0.007 mm^2 of "granules" 3.53 mm^2 of lamina propria, 0.005 mm^2 of "collagen", 6.55 mm^2 of "mature/surface epithelial layer", and 4.82 mm^2 of basal epithelial layer") were annotated for the model training.

Our EoE AI model has the capability of performing automated analyses of all histological levels on a given slide or any specifically designated area (region of interest, ROI) for the following features: 1. Objects: eosinophils, lymphocytes, and squamous nuclei; 2. Semantic segmentation layers: total tissue area (excluding non-squamous mucosa and debris), squamous epithelium, epithelial layers (basal and surface), DIS, lamina propria, collagen tissue; and 3. instance segmentation layer (counted as objects and measured as area simultaneously): granules. Features were defined, for the purposes of this study, as follows:

Objects (Fig. 1):

Eosinophils: Nucleated cells showing typical eosinophilic granules within its cytoplasm were labeled as eosinophils. Scattered eosinophilic granules (i.e., "degranulated eosinophils") and clusters of granules (including collections of extravasated granules and tangentially sectioned eosinophils with no recognizable nuclei were excluded (see description of "granules" below).

Lymphocytes: Round or elongated cells with dark, homogeneous nuclei and scant, clear, non-granular cytoplasm, not fulfilling criteria for other cell types.

Squamous cell nuclei: Round to oval nuclei surrounded by amphophilic (basal layer) or eosinophilic to pale cytoplasm (superficial layer), often with visible nucleoli, typical of squamous cells.

Semantic segmentation features (Fig. 2):

Tissue: All tissue representing esophageal squamous mucosa. Gastric/columnar-type mucosa as well as small detached squamous and necrotic debris were excluded.

Basal layer (Fig. 3): Squamous cell layer along the deep aspect of the epithelium showing scant, dark/amphophilic cytoplasm, and inter-nuclear distance of up to 1 average squamous nuclear diameter (by pathologist's visual estimation).

Surface/mature layer (Fig. 3): Squamous cell layer along the superficial aspect of the epithelium showing abundant, eosinophilic to clear cytoplasm, with inter-nuclear distance greater than 1 average squamous nuclear diameter.

Spongiosis/DIS (Fig. 4): Any recognizable clear intercellular spaces between squamous epithelial cells, often showing recognizable intercellular bridges.

Lamina propria (Fig. 2): All subepithelial fibroconnective tissue, excluding muscularis mucosa smooth muscle.

Table 1
EoE AI model layers and classes. Abbreviations: EoE, eosinophilic esophagitis.

AI model layer	AI model class	Morphological feature detected	Output
1	Tissue	Total esophageal mucosal tissue, excludes columnar/non-squamous mucosa.	Tissue area, mm^2
2	Intercellular edema	Intercellular edema within epithelium (mature and basal), or dilated intercellular spaces (DIS)	Edema area, mm^2
	Granules	Eosinophilic granules from eosinophils (degranulation), eosinophil cytoplasmic fragments without a nucleus	Granules area, mm^2 and count
3	Surface layer	Mature squamous epithelial layer, including "prickle layer"/stratum spinosum and surface layer	Mature epithelium area, mm^2
	Basal layer	Basal zone of the esophageal squamous epithelium, where nuclei are separated by a distance of up to the diameter of their nuclei	Basal epithelium area, mm^2
	Lamina propria	Subepithelial connective tissue superficial to muscularis mucosae; excludes smooth muscle tissue and dense lymphoid aggregates	Lamina propria area, mm^2
4	Collagen	Individual collagen fibers or bundles	Collagen area, mm^2
5	Eosinophils	Nucleated eosinophils within epithelium (mature and basal)	Count
	Lymphocytes	Lymphocytes within epithelium (mature and basal)	Count
	Squamous nuclei	Nuclei of the epithelial cells	Count

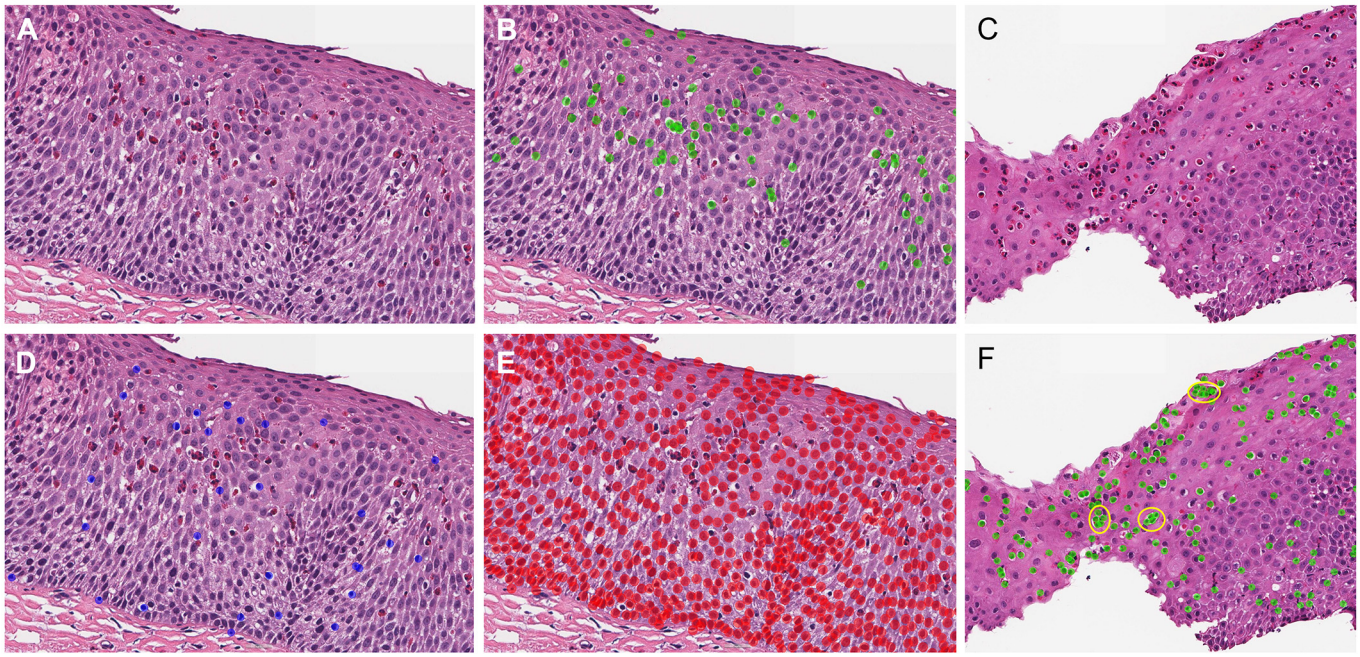

Fig. 1. Cell recognition feature of the EoE AI model. A, original H&E stain (100x magnification) showing eosinophil-rich infiltrate in a case of eosinophilic esophagitis; B, D, and E, automated recognition of eosinophils (B, green dots), lymphocytes (D, blue dots), and squamous nuclei (E, red dots). C, H&E stain of a case of EoE with eosinophilic abscesses; F, automated recognition of eosinophils and identification of eosinophilic abscesses by spatial analysis (yellow circles). Abbreviations: H&E, hematoxylin and eosin.

Collagen (Fig. 5): Pink/hyaline collagen fibers of any texture or thickness, located within the lamina propria.

Instance segmentation:

Granules: Any scattered granules (degranulation) or anucleated fragments recognizable as eosinophil cytoplasm.

Features recognized based on spatial analysis:

Eosinophilic abscesses (Fig. 3): Recognized as 4 or more eosinophils within a cluster, as defined by distance analysis (center-to-center distance of 20 μm or less between cells).

High power field-based analysis:

Since many of the histopathological parameters in the setting of EoE are expressed in terms of number of cells per high power field (HPF), our model was designed to include the tessellation of WSIs into tiles of customizable sizes using R statistical software[8] in combination with images extracted from the Aiforia platform. We have adopted 0.24 mm^2 area (calculated from a field number of 22 and 400x objective, representing the microscope setup used by pathologists in our service) as our standard HPF for the purposes of this study. Tessellation was performed using two different methods: a) square tile method and b) Voronoi method. In the square tile method, tiles measuring 0.24 mm^2 were used over areas of the slide or

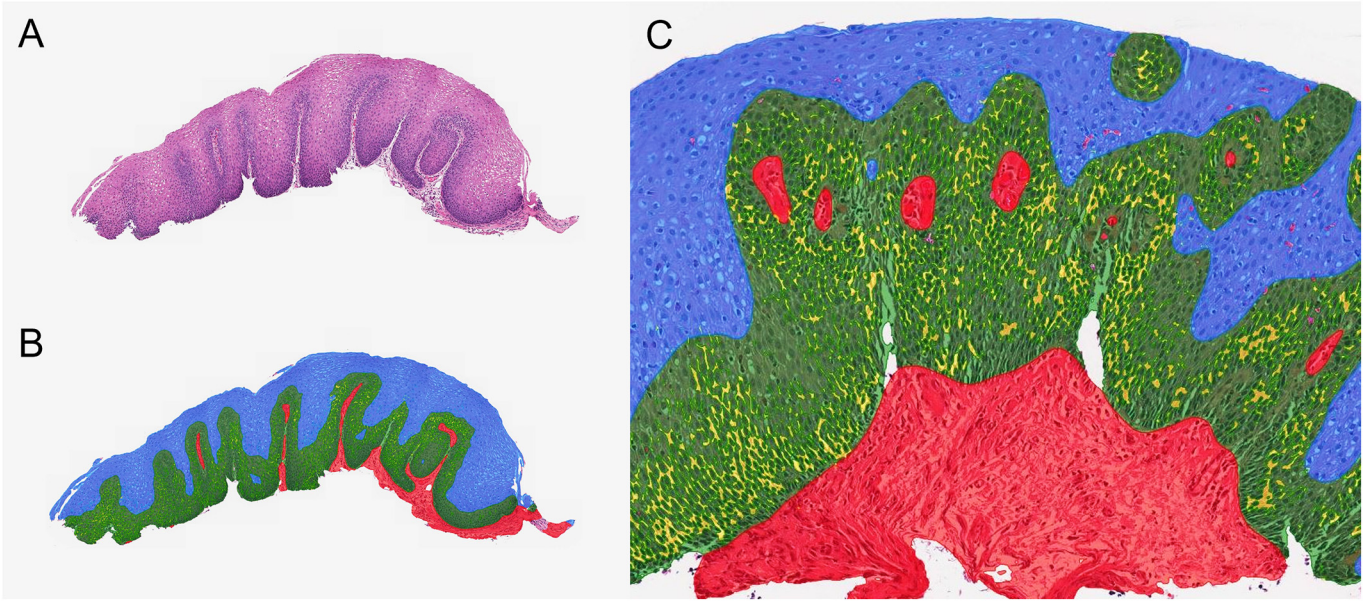

Fig. 2. Histologic layers of the squamous mucosa recognized by the EoE AI model. A, original H&E stain (20x magnification); B and C, automated layer segmentation (blue, superficial/mature squamous epithelium; green, basal layer; yellow, spongiosis/dilated intercellular spaces; and red, lamina propria); original magnification (B, 20x; C, 200x). Abbreviations: H&E, hematoxylin and eosin.

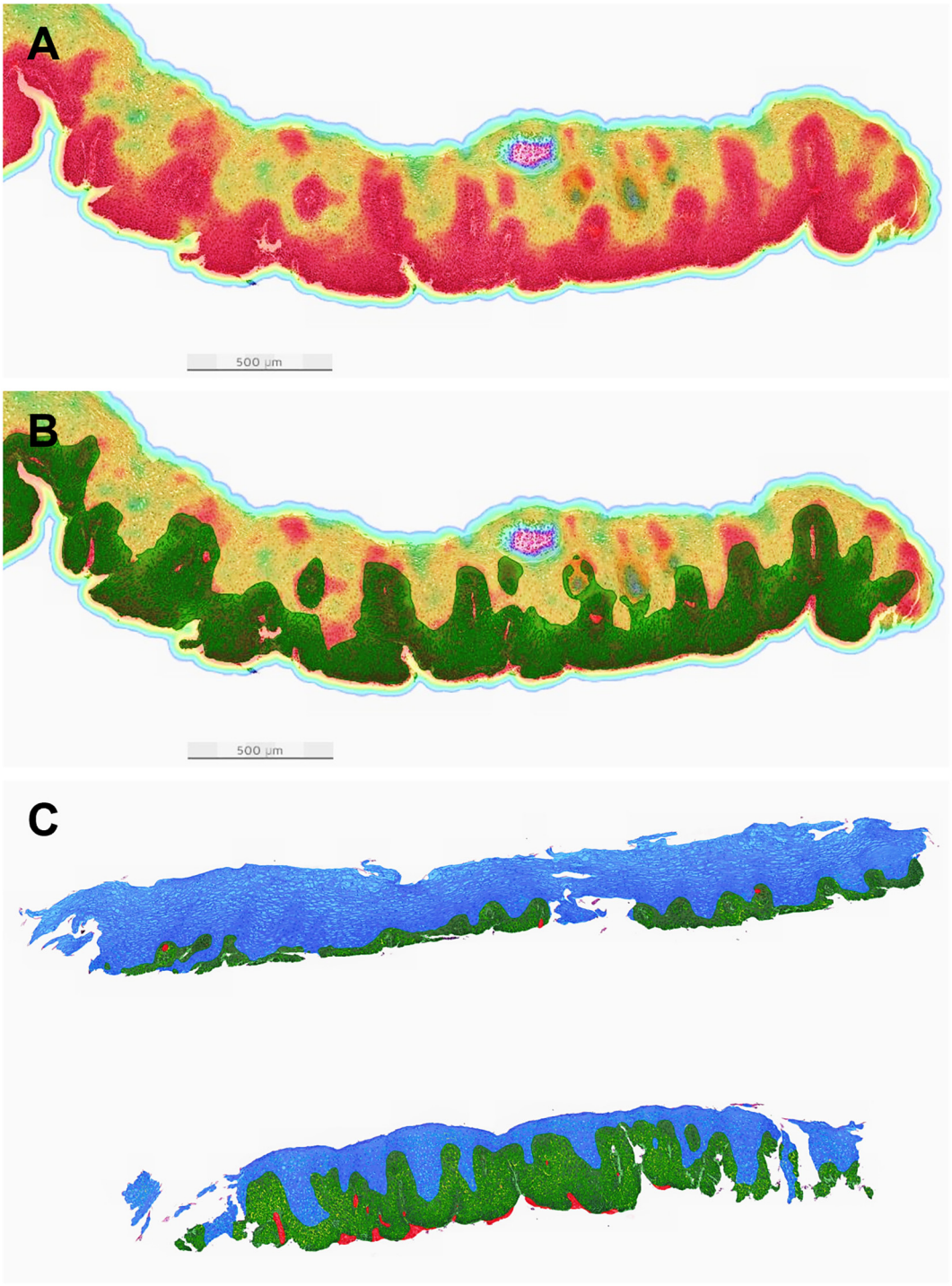

Fig. 3. Basal zone hyperplasia. A, heatmap of squamous nuclei showing highest density along the base of the epithelium (red), closely correlated to the distribution of basal layer (green) as recognized by the EoE AI model (inter-nuclear distance of up to 1 average squamous nuclear diameter, approximately) (B). C, an example of a normal fragment of esophageal squamous mucosa (above) in contrast with a fragment showing moderate basal zone hyperplasia (below) in the same biopsy sample (blue, mature/superficial squamous layer; green, basal layer).

ROI containing tissue, in a manner that all tissue was covered by tiles and that all tiles contained some tissue (Fig. 6A–D). Given that tiles may contain different amounts of tissue, concentration analyses using this type of tessellation can be performed both in an unadjusted (i.e., not taking into account the % area of each tile occupied by tissue) or adjusted (i.e., correcting for the % area of tissue) manner. In the Voronoi method, only the tissue area *per se* in each slide or ROI is included in the analysis and each tissue fragment is divided into areas approximating 0.24 mm^2 as much as possible, using Voronoi diagrams (Fig. 6E). Although the precise area per HPF is not uniform using the Voronoi method, calculation of cell density is corrected to reflect a standard denominator of 0.24 mm^2. Analyses of all objects/cell types and semantic segmentation features, therefore, can be performed on a per HPF basis, in addition to on a per ROI or whole slide basis.

Grading and staging of various features were possible by using the different methods of tessellation described above. For grading (i.e., maximal concentration of a given cell type in 1 HPF), the highest count within a single HPF was recorded for each slide using the square tile and Voronoi methods. For staging, the percentage of all HPF showing values above a

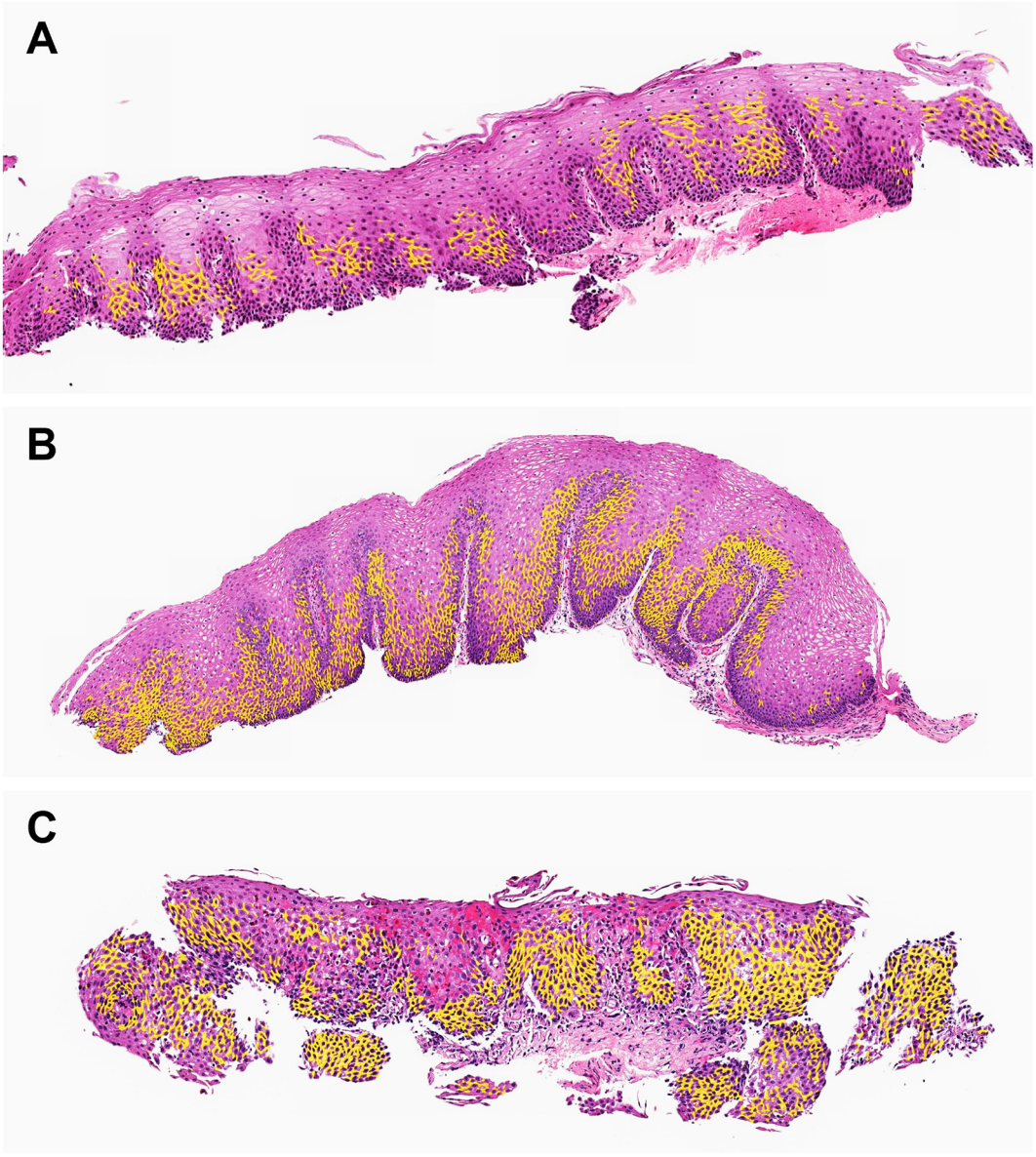

Fig. 4. Example of spongiosis (yellow) in esophageal squamous epithelium – mild (A), moderate (B), and severe (C). Hematoxylin and eosin stain, original magnification 20x.

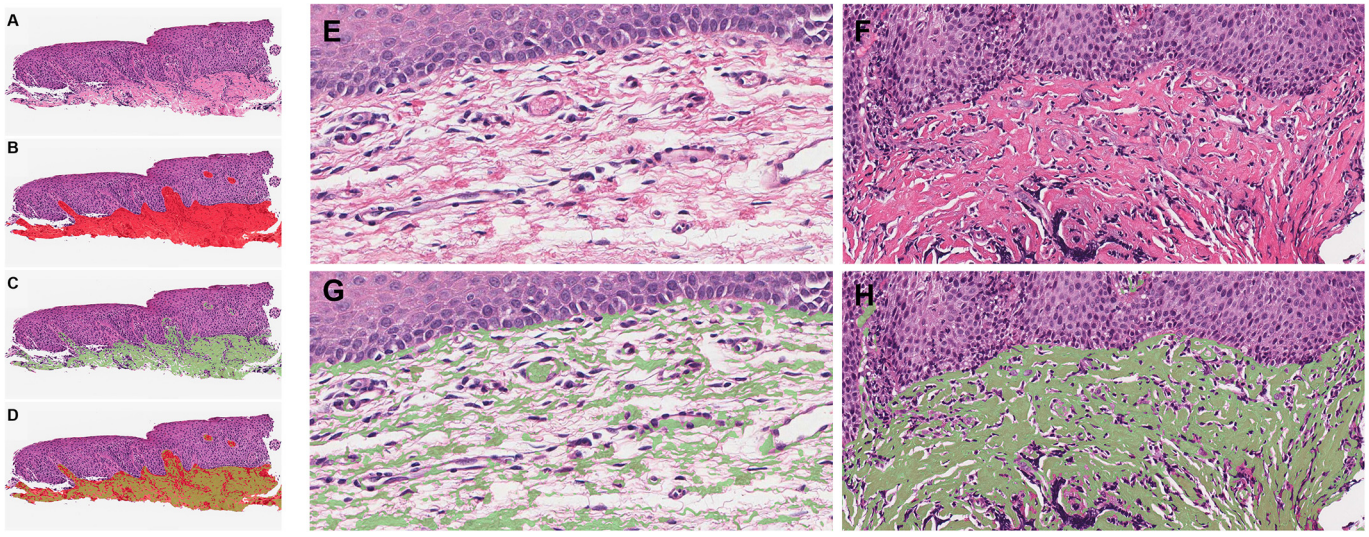

Fig. 5. Assessment of lamina propria and collagen by the EoE AI model. A, original H&E stain (20x magnification) of a case of EoE showing lamina propria with fibrosis; B, segmentation of lamina propria; C, segmentation of collagen within lamina propria; and D, superposition of lamina propria and collagen (ratio of lamina propria area/collagen area = fibrous tissue density score). E and G, example of normal lamina propria. F and H, example of fibrotic lamina propria in a case of EoE.

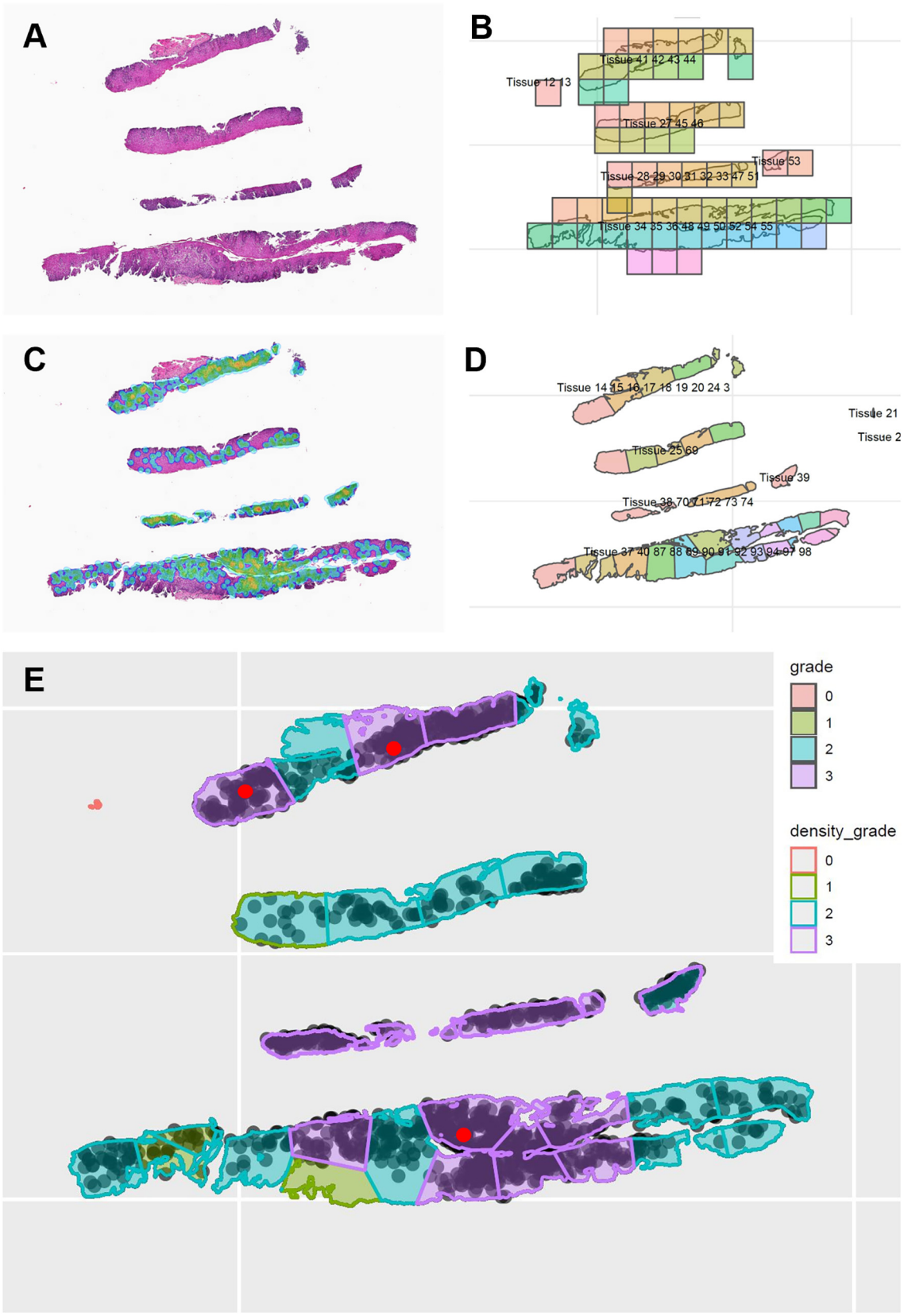

Fig. 6. Tesselation of biopsy fragments into high power fields (HPF) for digital analysis with the EoE AI model. A, Original H&E slide (20x magnficiation); B, grid system subdividing the tissue fragments into tiles measuring 0.24 mm^2; C, heatmap of the biopsy showing areas of highest concentration of eosinophils; D, biopsy fragments subdivided into areas of approximately 0.24 mm^2 using a method based on Voronoi diagrams. E, Voronoi tessellation method showing HPF regions and grade of each region (eosinophilic abscesses recognized as red dots).

Table 2
Scoring system for model performance of semantic segmentation features, compared to visual evaluation by specialized gastrointestinal pathologists.

Score	Model performance
1	Perfect or near-perfect accuracy (95%–100%, no significant errors)
2	Very good accuracy (80%–94%, only minor errors)
3	Good accuracy (70%–79%, significant errors but still captures the feature well)
4	Insufficient accuracy (below 70%, does not capture the feature to a useful level)

certain threshold (e.g., 15 for eosinophils) for counts or percent area (e.g., 20% for basal zone hyperplasia) for a given feature was used.

All object and instance segmentation features in our AI model can also be studied using spatial analysis. Center-to-center distances are used for object features (e.g., all cell types) and center-to-center, center-to-edge, or edge-to-edge distances can be used for features recognized by instance segmentation (e.g., granules). Due to this capability, eosinophilic abscesses could be identified using spatial analysis of objects (eosinophils in this case) alone, circumventing the necessity of recognition of this parameter as an independent feature. Nearest neighbor distance can also be obtained for all object and instance segmentation features, which, in turn, can be used to calculate various clustering/distribution indexes (e.g., Hopkins Statistics, clustering value, etc) within each fragment, ROI, or whole slide.

Intra-model reproducibility

Twelve digital slides (2 diagnosed as normal and 10 with varying grades of eosinophilia and epithelial injury) were selected. The reproducibility of the EoE AI model was assessed in several different ways, including repeat analysis of the same digital slide, analysis of a repeat scan of the same slide by the same scanner, and separate analyses of different histologic sections within the same slide and on separate slides (i.e., consecutive histologic sections). The impact of these factors on the assessment of each histologic feature by our model was evaluated.

Assessment of accuracy of feature recognition by the model

A subset of 759 objects (105 eosinophils, 517 squamous nuclei, and 137 lymphocytes) in a total of 110 validation regions within 6 digital slides in the dataset was reserved as independent "test sets" in order to assess the validity of the AI model outside the training set. Trained AI models were validated using the Analytical Validation modules of our platform. Five specialized gastrointestinal pathologists used integrated annotation tools to score the same criteria as the AI model on the reserved test set, in a blind and independent manner. A separate independent test set of 213 ROIs within 10 slides (727 eosinophils) was also analyzed for eosinophils only by a single central GI pathologist. The resulting analysis yielded an inter-operator agreement report for both human–human and human–AI comparison, with total error %, false positive %, false negative %, precision, sensitivity, and their harmonic mean as the F1-score. These results were used to assess the AI performance in relation to human performance, e.g., determination of superiority or non-inferiority for every specific object feature (i.e., cell types). Semantic segmentation features were also assessed by 5 independent pathologists. Specific areas (19 validation regions of interest [ROI] within 9 digital slides) representing the full spectrum of histologic changes related to each feature of interest were presented to validators, who were able to visually inspect exactly how the model performed. The AI model's accuracy was rated according to the criteria shown in Table 2.

Statistical analysis

Performance data (sensitivity, specificity, precision, F1-score, error rate, false-positive rate, false-negative rate) was calculated for both pathologists and AI model. The normality of the distribution of the time variable was examined using the Shapiro–Wilk normality test. Average and standard deviation were used for normally distributed data; otherwise, median and interquartile range were used. Statistical analyses were performed using MedCalc Statistical Software version 19.2.6 (MedCalc Software Ltd, Ostend, Belgium).

Results

The AI model showed a fairly high accuracy in the recognition of most histologic features in the spectrum of EoE, with F1 scores of >90% for the majority of features. The performance of the model for each feature compared to original annotations are described in Table 3. The performance of the AI model for all cell type features was similar/non-inferior to that of our group of GI pathologists (F1-scores: 94.5–94.8 for AI vs human and 92.6–96.0 for human vs human). Result details are shown in Table 4. The additional larger independent test set analyzed for eosinophils only by a single central pathologist yielded F1-score of 89.2, false-positive rate of 10.4%, false-negative rate of 12.1%, and precision of 92.1% (AI vs central pathologist).

Segmentation area features were rated for accuracy using the following scale: 1. "perfect or nearly perfect" (95%–100%, no significant errors), 2. "very good" (80%–95%, only minor errors), 3. "good" (70%–80%, significant errors but still captures the feature well), 4. "insufficient" (less than 70%, significant errors compromising feature recognition). Rating scores for tissue (1.01), spongiosis (1.15), basal layer (1.05), surface layer (1.04), lamina propria (1.15), and collagen (1.11) were in the "very good" to "perfect or nearly perfect" range, while degranulation (2.23) was rated between "good" and "very good".

Intra-model reproducibility

Re-analysis of 12 esophageal biopsy digital slides with our EoE AI model resulted in less than 0.1% difference for all object counts and semantic segmentation area measurements. When 2 consecutive slides from the same paraffin tissue block (each containing 3 consecutive tissue levels) were

Table 3
Performance of the EoE AI model for each feature compared to training annotations. Abbreviations: DIS, dilated intercellular spaces.

Feature/layer	False positive	False negative	Precision	Sensitivity	Specificity	F1-score
Tissue	0.2%	0.1%	99.2%	99.5%	99.2%	99.3%
All sublayers	0.4%	1.6%	97.9%	92.5%	99.6%	95.1%
Basal zone	2.7%	14.3%	96.8%	85.6%	97.3%	90.9%
Surface layer	1.5%	4.2%	98.4%	95.7%	98.5%	97.0%
Granules	30.2%	9.9%	74.9%	90.0%	69.8%	81.7%
DIS	52.0%	19.2%	60.8%	80.7%	48.0%	69.3%
Lamina propria	1.5%	4.2%	98.4%	95.7%	98.5%	97.0%
Collagen	3.1%	4.6%	96.8%	95.3%	96.9%	96.0%
All cells	1.2%	4.2%	98.7%	95.7%	98.8%	97.1%
Eosinophils	1.4%	11.5%	98.3%	88.4%	98.6%	93.1%
Lymphocytes	2.9%	3.6%	97.0%	96.3%	97.1%	96.7%
Squamous nuclei	1.1%	3.1%	98.8%	96.8%	98.9%	97.8%

Table 4
Abbreviations: AI, artificial intelligence (i.e., model); FP, false positive; FN, false negative.

	Eosinophils		Lymphocytes		Squamous nuclei	
	AI vs Human	Human vs Human	AI vs Human	Human vs Human	AI vs Human	Human vs Human
FP%	5.8%	4.3%	7.0%	9.7%	3.3%	5.9%
FN%	4.7%	3.6%	5.6%	7.2%	6.7%	4.7%
Error %	9.0%	6.8%	10.1%	13.2%	9.5%	9.5%
Precision%	95.2%	96.3%	94.5%	92.7%	96.8%	94.9%
Sensitivity %	95.2%	96.3%	94.3%	92.7%	93.2%	95.2%
Specificity %	94.1%	95.7%	93.0%	90.3%	96.7%	94.1%
F1-score %	94.8%	96.0%	94.5%	92.6%	94.7%	94.7%

compared, median difference in cell counts (whole slide analyses) ranged from 4% to 10%, while median difference in semantic segmentation areas ranged from 4% to 33%. When individual tissue levels within slides were analyzed separately, the median difference between consecutive levels (i.e., 4-μm distance between sections) ranged from 0.8% to 8.8% for cell counts and from 0.8% to 16.1% for semantic segmentation areas. Two-level difference in measurements (i.e., levels 8 μm apart) were 3.2%–7.1% for cell counts and 1.32%–24.4% for semantic segmentation areas. Finally, 5-level difference in measurements (levels 20 μm apart) were 6%–13.9% for cell counts and 4%–28.5% for semantic segmentation areas. Results are summarized in supplemental Tables 1 and 2.

Discussion

In this study, we have described the development and technical validation of a novel, supervised AI model for the evaluation of individual histopathologic features in the spectrum of esophageal mucosal eosinophilia. The goal of this study was to provide a "proof-of-principle" model in the setting of EoE – an AI model that could serve as a semi-automated tool for anatomic pathology, providing accurate, reproducible, quantitative assessment of various microscopic features of interest, increasing both efficiency and reporting standardization in this specific context.

The histologic evaluation of EoE is still, in practice, largely restricted to a traditional (i.e., unaided by digital tools) assessment of eosinophils by light microscopy. Pathologists are generally expected to provide an estimate of the highest concentration of eosinophils per HPF in a given sample.[3] Both parts of this apparently simple operation, however, present some meaningful challenges. The numerator – the counting of eosinophils – is predicated on: (1) clearly defining what is classified as an eosinophil (i.e., restricting the counting to nucleated cells or not), (2) correctly identifying the slide, level, fragment, and precise area of highest eosinophils concentration, and (3) performing the actual counting correctly. The denominator – a HPF – also represents an important contributor in the issue of interobserver variability, as its area may vary over 3-fold depending on the field diameter of different microscope manufactures and eyepiece specifications (ranging from 0.13 to 0.37 mm^2).[9] In 2017, a more comprehensive scoring system, the EoEHSS, has been proposed and shown to be fairly reproducible. In contrast to PEC, the EoEHSS also includes assessment of various features of epithelial injury as well as subepithelial fibrosis.[5,6]

We believe our AI model represents an improvement over the currently utilized methods in a few different ways. The classification of eosinophils as "objects" in our platform allows for detailed analysis of their number, density, and localization within the tissue. Our model can yield results for the concentration of eosinophils within different epithelial layers (basal layer vs surface), measure density of any cell of interest on a HPF basis and can also assess their two-dimensional spatial distribution (by various methods of clustering analysis). One obvious application of spatial analysis, which was utilized in our model, is the detection of eosinophilic abscesses (defined as 4 or more eosinophils clustered within a pre-defined distance from one another).

Eosinophil degranulation is also a feature of interest in the setting of EoE, defined here as structures ranging from fine discohesive eosinophilic granules scattered throughout the tissue to larger clumps of anucleated eosinophil cytoplasm (i.e., not meeting our definition of "eosinophil", which required the presence of a nucleus). This feature presents some challenges from a technical standpoint, as the degree of contrast with other structures, such as red blood cell fragments and the eosinophilic/slightly granular cytoplasm of squamous cells, can be fairly low. In our model, this feature is classified as "instance segmentation" and, as such, can be analyzed in terms of numbers (i.e., as an object) or in terms of area (i.e., as semantic segmentation). This way, if one wishes to classify larger cytoplasm fragments as "eosinophils", as advocated by some pathologists, this would be possible (post-analytically) without the need to modify the algorithm.

Our model also has the capability of recognizing lymphocytes, which is a histologic feature that is not routinely evaluated or quantified, but that may be of interest in this setting (as well as in the evaluation of cases in the spectrum of "lymphocytic esophagitis).[10–14] Squamous nuclei are also recognized by the model and may serve as a useful denominator for quantitative analyses of different features.

Basal layer hyperplasia is perhaps the main histologic indicator of epithelial tissue injury in the esophageal mucosa and is most commonly defined as a basal layer occupying >15%–20% of the epithelial thickness.[6,15] Although this binary assessment is easily available, the simple recognition of the basal layer and its quantitative analysis throughout the sample, as in our current model, largely obviate the need for a specific cutoff for "basal zone hyperplasia". During the annotation phase, the inter-nuclear distance (between squamous nuclei) of up to 1 average squamous nuclear diameter was used as a general guide to the visual recognition of basal (vs mature/superficial) zone.

Dilated intercellular spaces (DIS), also known as spongiosis or intercellular edema, represents another important feature of esophageal squamous epithelial injury, whereby the normally narrow intercellular spaces become dilated, filled with edematous fluid, and intercellular bridges (desmosome intercellular processes) become discernible by light microscopy.[16–18] DIS is thought to represent a morphologic manifestation of key steps in the pathogenesis of EoE – namely, abnormalities in intercellular junction proteins/epithelial barrier – leading to increased epithelial permeability. Our model has the capability of recognizing and quantifying this otherwise difficult-to-assess histologic feature, albeit with a higher error rate compared to most other features. The relatively low specificity of our model in detecting this feature compared to training annotations is likely related to the relatively large ratio between the annotated areas of DIS and the (small) ROIs used in its evaluation. This is supported by the fact that the visual inspection of DIS segmentation by GI pathologists was rated between the "very good (score of 2)" and "perfect/nearly perfect (score of 1)" categories, with an average score of 1.15.

Our model is capable of accurately recognizing lamina propria/subepithelial tissue. Given the importance of fibrosis in the context of EoE,[19–23] the ability to specifically evaluate for abnormalities within this compartment is a relevant attribute. One of the challenges in evaluating fibrosis in this setting, however, is establishing the difference between normal fibrous tissue (and its range in appearance according to patient age, location within the esophagus, subepithelial depth, etc) and *bona-fide* fibrosis.[21] Considering this, we have trained our model to simply recognize individual collagen bundles, at least to the extent that this is feasible histologically and is within the capability of our current platform. Therefore, within the subepithelial compartment, collagen tissue is specifically recognized regardless of its histological "texture", but inter-collagen gaps, edematous interstitial spaces, blood vessels, inflammatory cells, muscle tissue, etc., are excluded. The ratio between collagen area and total lamina propria area is then used as a fibrosis (or fibrous tissue) score within a given sample.

In addition, with precise tissue recognition, and specific segmentation of the histologic layers of the squamous mucosa, our model can accurately subdivide the appropriate areas of the sample into "standard" area units for

the purposes of counting cells or any other analytical task. In our current settings, our "HPF" is defined as 0.24 mm^2 (representing the standard HPF area of microscopes in our practice, an average HPF area amongst the most common manufactures and a criterion used in previous studies);[6] however, this is a customizable parameter that can easily be adjusted, if necessary. Since the entire tissue can be analyzed with our model (all levels and/or slides), the region of highest concentration of eosinophils (or any other object or semantic segmentation feature of interest) is guaranteed to be properly identified, and all recognized cells of interest properly counted, limited only by the accuracy of the model in recognizing the features themselves.

Since our model has been designed to analyze tissue areas on the basis of pre-defined individual HPF areas, features of interest can be both "graded" (i.e., described in terms of the most affected a single HPF) and "staged" (i.e., described in terms of average involvement of all HPFs, percent of HPF areas with any involvement, or similar distribution metric). Although this may represent a significant improvement compared to our currently utilized non-digital histopathologic method, analyzing slides for grade/stage on a HPF basis presents some technical challenges to be overcome. In our model, we have applied 2 different digital strategies to approach this problem – one that tessellates the tissue into square tiles (similar to what has previously been done in other settings)[24] and one novel application of Voronoi diagrams which attempts to divide irregular tissue fragments into areas approximating a standard HPF as much as possible. Both strategies can yield values that are adjusted for percent of tissue within the tile (square tile method) and for tile size (Voronoi method). Both approaches have advantages and limitations. Most meaningfully, the unadjusted square tile method is conceptually the most similar to what pathologists currently do (i.e., analysis of a HPF area showing the highest concentration of eosinophils, regardless of whether a certain percentage of "empty spaces" area is present within the field of view). Preliminary analysis by our group showed that this method indeed has the closest correlation with PEC performed using the traditional method (unpublished data).

To our knowledge, this is the first AI model ever designed specifically for the assessment of EoE/mucosal eosinophilia-related histologic findings. Future efforts should be directed towards improved recognition of eosinophil granules, more comprehensive evaluation of subepithelial collagen patterns, as well as capability to recognize additional features such as dyskeratosis, surface epithelial change, and neutrophilic infiltrate. Moreover, models that have the capabilities of accurately evaluating a wide range of H&E stains (of varying quality, variable staining characteristics, and from different laboratories) and analyzing WSIs from different scanners – an objective that was beyond the scope of our project – would be both useful and desirable. Nevertheless, we believe the current model represents a successful proof-of-concept, a potential blueprint for subsequent models, as well as an important step in the semi-automation and standardization of the histologic analysis of features in the spectrum of esophageal mucosal eosinophilia.

Funding

This work was supported by internal funding, Division of Anatomic Pathology, Mayo Clinic, Rochester MN.

Declaration of interests

The authors declare that they have no known competing financial interests or personal relationships that could have appeared to influence the work reported in this paper.

Acknowledgments

NA.

Appendix A. Supplementary data

Supplementary data to this article can be found online at https://doi.org/10.1016/j.jpi.2022.100144.

References

1. Attwood SE, Smyrk TC, Demeester TR, Jones JB. Esophageal eosinophilia with dysphagia. A distinct clinicopathologic syndrome. Dig Dis Sci 1993;38(1):109–116.
2. Straumann A, Spichtin HP, Bernoulli R, Loosli J, Vogtlin J. Idiopathic eosinophilic esophagitis: a frequently overlooked disease with typical clinical aspects and discrete endoscopic findings. Schweiz Med Wochenschr 1994;124(33):1419–1429.
3. Ma C, Schoepfer AM, Dellon ES, Bredenoord AJ, Chehade M, Collins MH, et al. Development of a core outcome set for therapeutic studies in eosinophilic esophagitis (COREOS). J Allergy Clin Immunol 2022;149(2):659–670.
4. Collins MH. Histopathology of eosinophilic esophagitis. Dig Dis 2014;32(1–2):68–73.
5. Collins MH, Martin LJ, Alexander ES, Todd Boyd J, Sheridan R, He H, et al. Newly developed and validated eosinophilic esophagitis histology scoring system and evidence that it outperforms peak eosinophil count for disease diagnosis and monitoring. Dis Esophagus 2017;30(3):1–8.
6. Warners MJ, Ambarus CA, Bredenoord AJ, Verheij J, Lauwers GY, Walsh JC, et al. Reliability of histologic assessment in patients with eosinophilic oesophagitis. Aliment Pharmacol Ther 2018;47(7):940–950.
7. Pai RK, Bredenoord AJ, Feagan BG, Jairath V. Editorial: validating reliability of the eosinophilic oesophagitis histological scoring system (EOE-HSS)-an important first step. Authors' reply. Aliment Pharmacol Ther 2018;47(12):1714–1715.
8. Dessau RB, Pipper CB. "R"–project for statistical computing. Ugeskr Laeger 2008;170(5):328–330.
9. Bonert M, Tate AJ. Mitotic counts in breast cancer should be standardized with a uniform sample area. Biomed Eng Online 2017;16(1):28.
10. Genta RM. Lymphocytic esophagitis. Gastroenterol Hepatol (N Y) 2015;11(8):559–561.
11. Mandaliya R, Dimarino AJ, Cohen S. Lymphocytic esophagitis mimicking eosinophilic esophagitis. Ann Gastroenterol 2012;25(4):355–357.
12. Lisovsky M, Westerhoff M, Zhang X. Lymphocytic esophagitis: a histologic pattern with emerging clinical ramifications. Ann N Y Acad Sci 2016;1381(1):133–138.
13. Pasricha S, Gupta A, Reed CC, Speck O, Woosley JT, Dellon ES. Lymphocytic esophagitis: an emerging clinicopathologic disease associated with dysphagia. Dig Dis Sci 2016;61(10):2935–2941.
14. Truskaite K, Dlugosz A. Prevalence of eosinophilic esophagitis and lymphocytic esophagitis in adults with esophageal food bolus impaction. Gastroenterol Res Pract 2016;2016:9303858.
15. Odze RD. Pathology of eosinophilic esophagitis: what the clinician needs to know. Am J Gastroenterol 2009;104(2):485–490.
16. Cui R, Zhang H, Zhou L, Lu J, Xue Y, Wang Y, et al. Diagnostic value of dilated intercellular space and histopathologic scores in gastroesophageal reflux disease. Dis Esophagus 2015;28(6):530–537.
17. Ravelli A, Villanacci V, Cadei M, Fuoti M, Gennati G, Salemme M. Dilated intercellular spaces in eosinophilic esophagitis. J Pediatr Gastroenterol Nutr 2014;59(5):589–593.
18. Ravelli AM, Villanacci V, Ruzzenenti N, Grigolato P, Tobanelli P, Klersy C, et al. Dilated intercellular spaces: a major morphological feature of esophagitis. J Pediatr Gastroenterol Nutr 2006;42(5):510–515.
19. Hiremath G, Sun L, Correa H, Acra S, Collins MS, Bonis P, et al. Development and validation of web-based tool to predict lamina propria fibrosis in eosinophilic esophagitis. Am J Gastroenterol 2022;117(2):272–279.
20. Li-Kim-Moy JP, Tobias V, Day AS, Leach S, Lemberg DA. Esophageal subepithelial fibrosis and hyalinization are features of eosinophilic esophagitis. J Pediatr Gastroenterol Nutr 2011;52(2):147–153.
21. Chehade M, Sampson HA, Morotti RA, Magid MS. Esophageal subepithelial fibrosis in children with eosinophilic esophagitis. J Pediatr Gastroenterol Nutr 2007;45(3):319–328.
22. Aceves SS, Ackerman SJ. Relationships between eosinophilic inflammation, tissue remodeling, and fibrosis in eosinophilic esophagitis. Immunol Allergy Clin North Am 2009;29(1):197–211.xiii-xiv.
23. Armbruster-Lee J, Cavender CP, Lieberman JA, Samarasinghe AE. Understanding fibrosis in eosinophilic esophagitis: are we there yet? J Leukoc Biol 2018;104(1):31–40.
24. Ibrahim A, Lashen AG, Katayama A, Mihai R, Ball G, Toss M, et al. Defining the area of mitoses counting in invasive breast cancer using whole slide image. Mod Pathol 2022;35(6):739–748.